INTER-AMERICAN TROPICAL TUNA COMMISSION

SCIENTIFIC ADVISORY COMMITTEE

13TH MEETING

(by videoconference)
16-20 May 2022

DOCUMENT SAC-13 INF-K

STANDARDIZING THE PURSE-SEINE INDICES OF ABUNDANCE AND ASSOCIATED LENGTH COMPOSITIONS FOR SKIPJACK TUNA IN THE EASTERN PACIFIC OCEAN

Haikun Xu and Cleridy E. Lennert-Cody

SUMMARY

The staff is currently using an interim stock assessment to evaluate the stock status of skipjack tuna (SKJ) in the eastern Pacific Ocean (EPO). This assessment requires indices of abundance and length compositions for SKJ caught by the purse-seine fishery. SKJ in the EPO are harvested mainly by two types of purse-seine sets: sets on tunas associated with floating-objects (OBJ) and sets on unassociated schools of tuna (NOA). We fit two spatiotemporal models separately to catch and effort data from the OBJ and NOA sets to provide standardized OBJ and NOA indices of abundance for the interim stock assessment. The spatiotemporal models use an area-weighting approach to compute indices of abundance. They can estimate spatial autocorrelations and use that information to impute fish abundance in unfished locations according to neighboring catch-per-unit-effort (CPUE) data. Also, they can model differences in fishing efficiency among purse-seine vessels (vessel effects) and remove this source of variability from the standardized abundance index. The length composition estimates associated with the two standardized indices of abundance are also provided. These are computed by raising the sample length-frequency distributions using the standardized CPUE predicted by the spatiotemporal models. The estimates of indices of abundance and length compositions are based on the CPUE and length-frequency data collected in the EPO, so they represent the abundance trend and length composition of the EPO-wide SKJ population.

1. BACKGROUND

Indices of relative abundance are key inputs to a stock assessment model as they directly inform the model about how population abundance changes over time (Francis 2011). SKJ in the EPO are harvested mainly by two types of purse-seine sets: sets on tunas associated with OBJ and sets on unassociated NOA (SAC-12-03). The indices of relative abundance are usually assumed in the stock assessment model to be proportional to population abundance (Maunder and Punt 2004). Ideally, indices of abundance should be computed using fishery-independent survey data, which have a random or fixed sampling design in space and are collected using the same gear and mode of fishing (operational characteristics) through time to assure constant catchability and selectivity. For SKJ in the EPO, however, fishery-independent survey data are not available due to the high cost and logistical challenge of implementing a fishery-independent survey in an area as large as the EPO. Therefore, the OBJ and NOA indices of abundance for SKJ depend solely on fishery-dependent CPUE data.

An ideal measure of effort to use for CPUE-based indices of abundance is not available for SKJ in the purse-seine fishery. Vessels that catch SKJ typically use both set types and the proportion of each set type used

may differ among vessels and differ among years for any given vessel. Catch-per-day-fished has been used in previous assessments of SKJ, but proportioning the days fished to each set type is considered unreliable and therefore is no longer used. In this analysis, we use number of sets as the measure of effort. This assumes that the size of the catch in a set (e.g. school size) changes in proportion to abundance.

We use a spatiotemporal model to standardize fishery-dependent CPUE data. Fishery-dependent CPUE data are not randomly distributed in space. They tend to concentrate in areas where fish abundance is high or fishing operations are easy to conduct (this phenomenon is referred to as preferential sampling). As such, it is not uncommon that fishery-dependent CPUE data within a quarter or even a year do not cover the entire spatial domain of interest. Based on the assumption that the CPUE of neighboring areas is more similar than the CPUE of areas separated by large distances, spatiotemporal models can use estimated spatial autocorrelations to impute fish abundance in unfished locations by borrowing neighboring CPUE data (Thorson *et al.* 2020). We use the spatiotemporal model also to remove the impact of factors other than population abundance (e.g., vessel-specific differences in fishing efficiency) on CPUE so that the standardized abundance index can be considered approximately proportional to population abundance. This paper describes the methodology used to estimate the OBJ and NOA indices of abundance and the associated length compositions for SKJ in the EPO that are used in the interim stock assessment (SAC-13-07).

2. DATA

2.1. Indices of abundance

Per-vessel set type-specific data on catch (in metric tons) and effort (in number of sets) of purse-seine vessels are used to estimate standardized OBJ and NOA indices of abundance for SKJ in the EPO. This dataset covers 2000-2021 and has a spatial and temporal resolution of 1° x 1° square and 1 day, respectively. In addition to location and time, the dataset also includes a unique vessel identifier for each purse-seine set. The data used in this analysis were collected by onboard observers of the Agreement on the International Dolphin Conservation Program observer program or obtained from vessel logbooks. Observer coverage of the purse-seine fishery has been largely limited to Class-6 vessels (fish carrying capacity > 363 t) and has been at or nearly 100% during 2000-2021 (Joseph 1994; Scott *et al.* 2016). Logbook data were used for trips of large purse-seine vessels for which no observer data were available and for trips of most Class 1-5 purse-seine vessels ($\leq$ 363 t fish carrying capacity).

For CPUE standardization, we fit the spatiotemporal models to the catch and effort data from only Class-6 purse-seine vessels. The main reasons for restricting the source of data to only large purse-seine vessels are: 1) Class-6 purse-seine vessels have higher observer coverage than Class 1-5 purse-seine vessels, which are not sampled by a formal fleet-wide observer program; 2) Class-6 purse-seine vessels operate across the tropical EPO while Class 1-5 purse-seine vessels operate primarily in the inshore region of the EPO (SAC-08-06a); and, 3) Class-6 purse-seine vessels likely have different fishing strategies than Class 1-5 purse-seine vessels (SAC-10 INF-K). We also restrict the spatial domain of the catch and effort data to the "core" fishing ground for SKJ (Figure 1), which we define for the OBJ and NOA fisheries as all 1° x 1° squares in the EPO with at least 11 and 6 years of CPUE data between 2000-2021, respectively.

2.2. Length compositions

Per-vessel set type-specific data on the length frequencies of SKJ caught by purse-seine vessels, in combination with the standardized CPUE from VAST, are used to provide OBJ and NOA length composition estimates associated with the indices of abundance. The length-frequency data covers 2000-2021 and has a spatial, temporal, and length resolution of 5° x 5° square, 1 month, and 1 cm, respectively. The data were collected by the IATTC port-sampling program. The collection of port-sampling data in 2020 was severely impacted by the COVID-19 pandemic, particularly in several ports where much of the bigeye tuna

catch is typically unloaded (SAC-13 INF-L). The collection of port-sampling data in 2021 was also impacted, although a full analysis of port-sampling data loss in 2021 has not yet been completed.

Length compositions for the indices of abundance should be raised by CPUE to reflect the length compositions of the population (Maunder *et al.* 2020). For the interim stock assessment, they are computed for each year-quarter by raising the raw length-frequency data by the standardized CPUE in the same spatiotemporal stratum for the same set type. The raising requires converting catch unit from weight to number of fish. We approximate this conversion by dividing the total catch amount by the estimated mean body weight for the same spatiotemporal stratum, which is not directly observed but calculated based on raw length-frequency observations and the length-weight relationship used in the interim stock assessment ($weight(kg) = 5.53 \times 10^{-6} \times length(cm)^{3.336}$). To be consistent with the data selection criteria for the indices of abundance, we also restrict the source of length composition data to Class-6 purse-seine vessels only. Also, only cells in the defined "core" fishing area for which length composition data are available are used in the analysis (i.e. a spatio-temporal model is not used to fill in areas without samples). The input sample size of length composition data is defined as the total number of wells sampled within a year-quarter.

3. SPATIOTEMPORAL MODELS

3.1. Indices of abundance

The abundance indices for SKJ in the EPO are standardized by a spatial delta-generalized linear mixed model (Thorson and Barnett 2017), which separately models encounter probability and positive catch rate to deal with zero-inflated catch rate data. The model uses the *logit* and *log* link functions for the linear predictors of encounter probability and positive catch rate, respectively. Both the encounter probability and positive catch rate model formulations in VAST include an intercept term (year-quarter effect), a spatial term, a spatiotemporal term, and a vessel effect term. The spatial and spatiotemporal terms are formulated as random effects. We use 100 (for OBJ sets) and 50 (for NOA sets) spatial knots to represent the spatial and spatiotemporal random effects, both of which are assumed to be autocorrelated in space following the Matérn function. The model accounts for vessel-specific differences in fishing efficiency through including a vessel effect term (estimated in VAST as a random effect), which is then removed when predicting standardized CPUE. VAST uses an area-weighting approach to compute standardized indices of abundance (see Xu *et al.* 2019 for more details).

The interim stock assessment uses the "quarters-as-years" approach and considered the period from 2000 to 2021 (the assessment ultimately started in the last quarter of 2005). To be consistent, the two spatiotemporal models treat the four quarters equally and have a quarterly time step from the first quarter of 2000 (model year 1) to the last quarter of 2021 (model year 88).

4. RESULTS

4.1. Indices of abundance

The two indices of abundance have similar interannual variations but differ in long-term trends. The OBJ index of abundance for skipjack does not have a noticeable long-term trend since 2000 while the NOA index of abundance for SKJ has a positive long-term trend during that period (Figure 2; Table 1).

According to the OBJ fishery in the EPO, SKJ density has a clear seasonal pattern (Figure 3). In the first quarter, the highest density of SKJ is found in the offshore tropical area (west of 120°W) and the inshore southern area. In the second quarter, this pattern still holds but SKJ density is generally lower throughout the EPO. In the third quarter, SKJ density increases in the inshore tropical area but decreases in the southern area to the lowest level within a year. In the fourth quarter, SKJ density increases greatly in the inshore tropical area, surpassing that in the rest of the EPO. Overall, the interannual variability of SKJ

density is larger in the inshore area than in the offshore area.

For the NOA fishery in the EPO, SKJ density does not appear to have a pronounced seasonal variation (Figure 4). Throughout the year, SKJ density is lowest in the inshore area north of 5°N, highest in the offshore tropical area west of 90°W, and relatively homogeneous in the rest of the NOA fishing ground.

4.2. Length compositions

Both the OBJ and NOA sets catch SKJ within the length range of 25 cm to 75 cm (Figure 5). In comparison to the OBJ sets, the NOA sets catch a higher proportion of large SKJ. This could be due at least partially to the difference in the spatial distribution of the two set types. In general, SKJ in the offshore area are smaller than those in the inshore area (SAC-13 INF-I). The NOA fishing ground is located to the east within the EPO, as compared to the OBJ fishing ground which extends to the EPO's western boundary (Figure 1). Therefore, the NOA sets are expected to catch proportionally more large SKJ than the OBJ sets. Both the sample sizes for OBJ and NOA length compositions, quantified as the number of wells sampled, show large interannual variations (Figure 6). Overall, the sample sizes for OBJ sets are pronouncedly larger than those for NOA sets, which may be due to several factors, including the greater number of OBJ sets made by the fleet as compared to NOA sets (SAC-13-03), and the extent to which NOA catch may be loaded into wells containing catch from other set types (wells with catch from multiple set types are not sampled by the port-sampling program; Suter 2010).

REFERENCES

Francis, R.I.C.C. 2011. Data weighting in statistical fisheries stock assessment models. Canadian Journal of Fisheries and Aquatic Sciences **68**(6): 1124-1138.

Joseph, J. 1994. The tuna - dolphin controversy in the eastern pacific ocean: Biological, economic, and political impacts. Ocean Development & International Law **25**(1): 1-30.

Maunder, M.N., and Punt, A.E. 2004. Standardizing catch and effort data: a review of recent approaches. Fisheries research **70**(2-3): 141-159.

Maunder, M.N., Thorson, J.T., Xu, H., Oliveros-Ramos, R., Hoyle, S.D., Tremblay-Boyer, L., Lee, H.H., Kai, M., Chang, S.-K., and Kitakado, T. 2020. The need for spatio-temporal modeling to determine catch-per-unit effort based indices of abundance and associated composition data for inclusion in stock assessment models. Fisheries Research **229**: 105594.

Scott, M.D., Lennert-Cody, C.E., Gerrodette, T., Skaug, H.J., Minte-Vera, C.V., Hofmeister, J., Barlow, J., Chivers, S.J., Danil, K., Duffy, L.M., Olson, R.J., Hohn, A.A., Fiedler, P.C., Ballance, L.T., and Forney, K.A. 2016. Data available for assessing dolphin population status

in the eastern tropical Pacific Ocean. Inter-Amer.Trop. Tuna Comm., Workshop on Methods for Monitoring the Status of Eastern Tropical Pacific Ocean Dolphin Populations: DEK-01 (Available at www.iattc.org/Meetings/Meetings2016/DEL-01/PDFs/_English/DEL-01_Data-Available-for-Assessing-Dolphin-Population-Status-in-the-Eastern-Tropical-Pacific-Ocean.pdf).

Thorson, J.T., and Barnett, L.A.K. 2017. Comparing estimates of abundance trends and distribution shifts using single- and multispecies models of fishes and biogenic habitat. ICES Journal of Marine Science **74**(5): 1311-1321.

Thorson, J.T., Maunder, M.N., and Punt, E. 2020. The development of spatio-temporal models of fishery catch-per-unit-effort data to derive indices of relative abundance. Elsevier. p. 105611.

Xu, H., Lennert-Cody, C.E., Maunder, M.N., and Minte-Vera, C.V. 2019. Spatiotemporal dynamics of the dolphin-associated purse-seine fishery for yellowfin tuna (Thunnus albacares) in the eastern Pacific Ocean. Fisheries research **213**: 121-131.

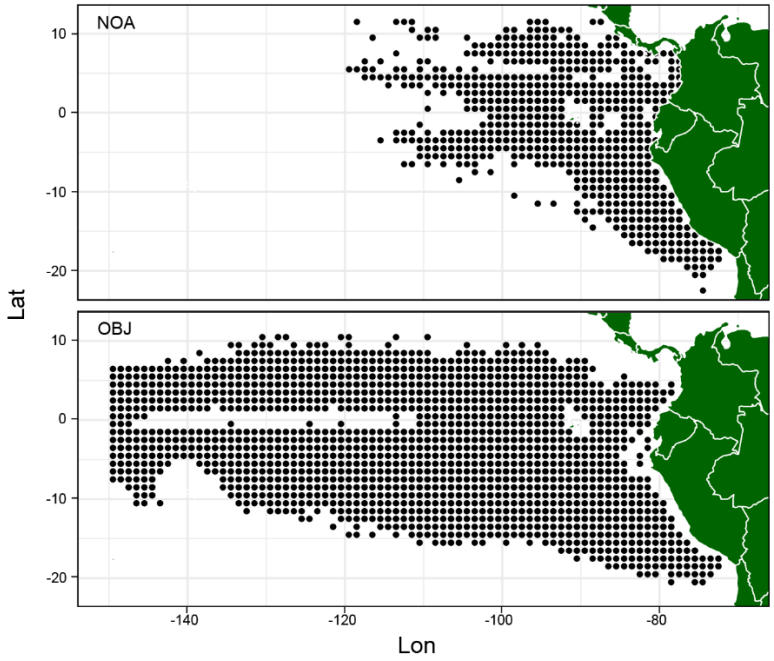

FIGURE 1. Spatial domains of catch and effort data used in the standardization of NOA (top) and OBJ (bottom) CPUE.

FIGURA 1. Dominios espaciales de los datos de captura y esfuerzo usados en la estandarización de la CPUE NOA (arriba) y OBJ (abajo).

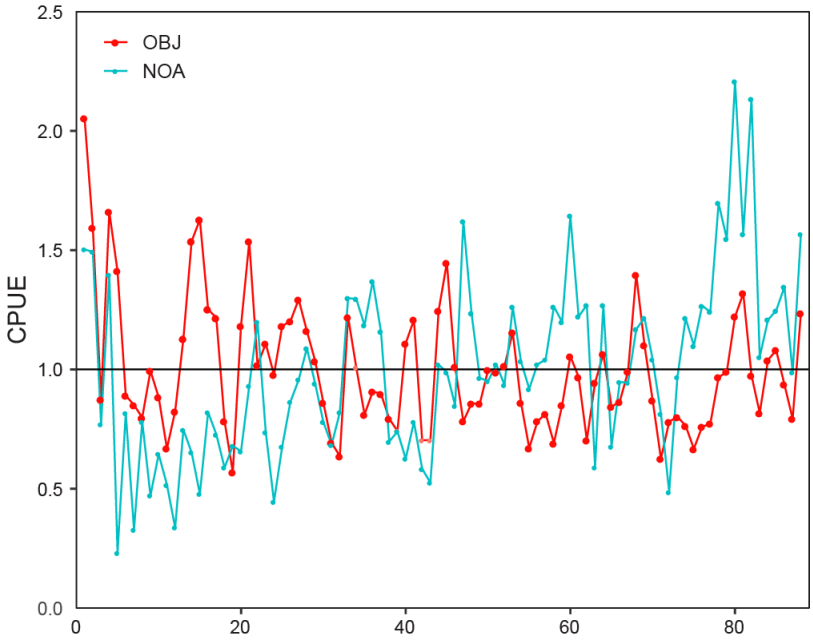

FIGURE 2. Time series of standardized OBJ and NOA indices of abundance for SKJ in the EPO.

FIGURA 2. Serie de tiempo de los índices de abundancia estandarizados OBJ y NOA para el SKJ en el OPO.

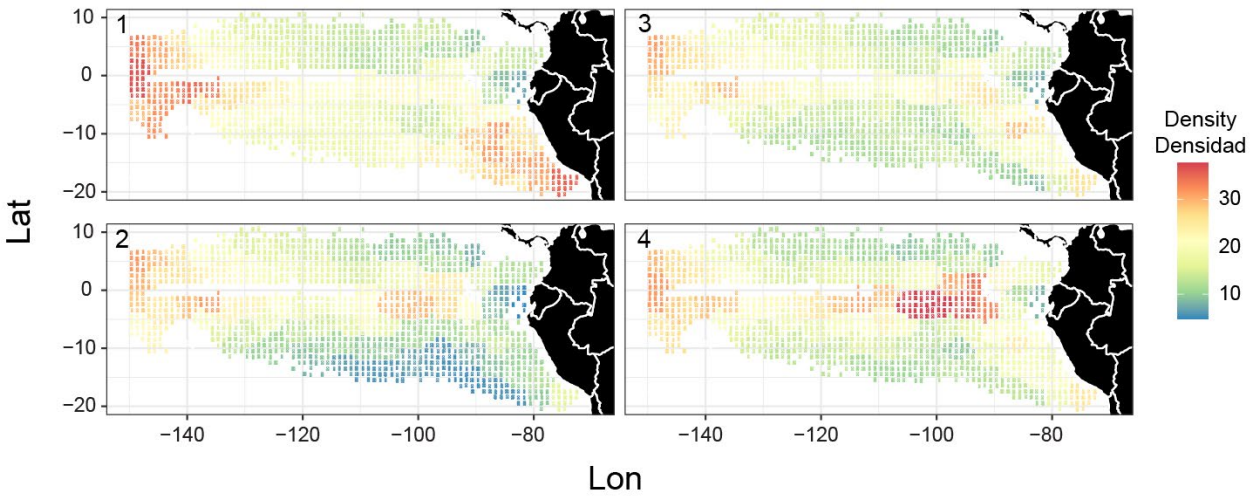

FIGURE 3. Quarterly spatial distribution of SKJ CPUE (tons per set) predicted by the spatiotemporal model fit to OBJ CPUE data.

FIGURA 3. Distribución espacial trimestral de la CPUE de SKJ (toneladas por lance) predicha por el modelo espaciotemporal ajustada a los datos de CPUE OBJ.

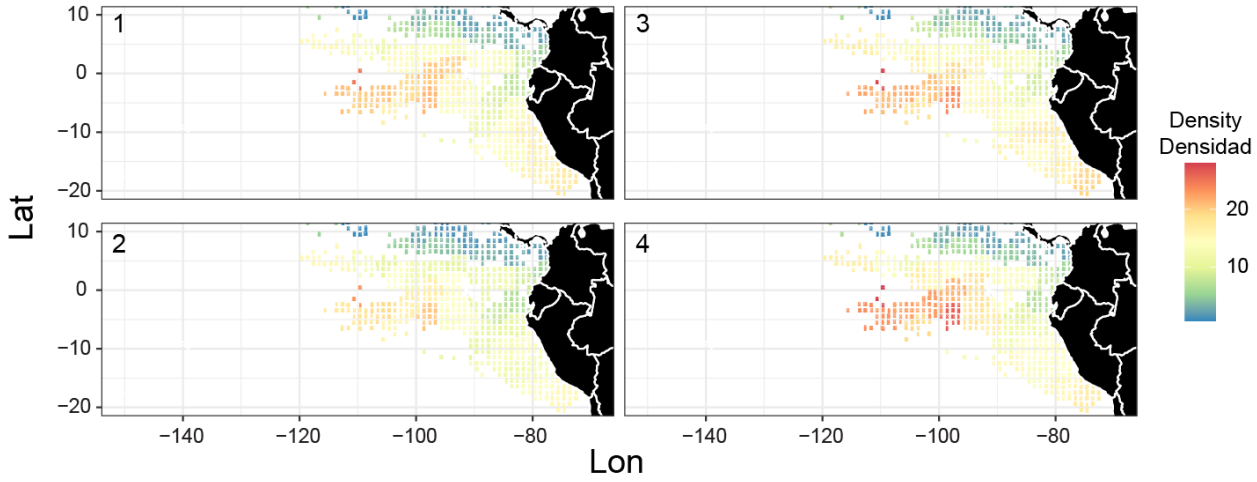

FIGURE 4. Quarterly spatial distribution of SKJ CPUE (tons per set) predicted by the spatiotemporal model fit to NOA CPUE data.

FIGURA 4. Distribución espacial trimestral de la CPUE de SKJ (toneladas por lance) predicha por el modelo espaciotemporal ajustada a los datos de CPUE NOA.

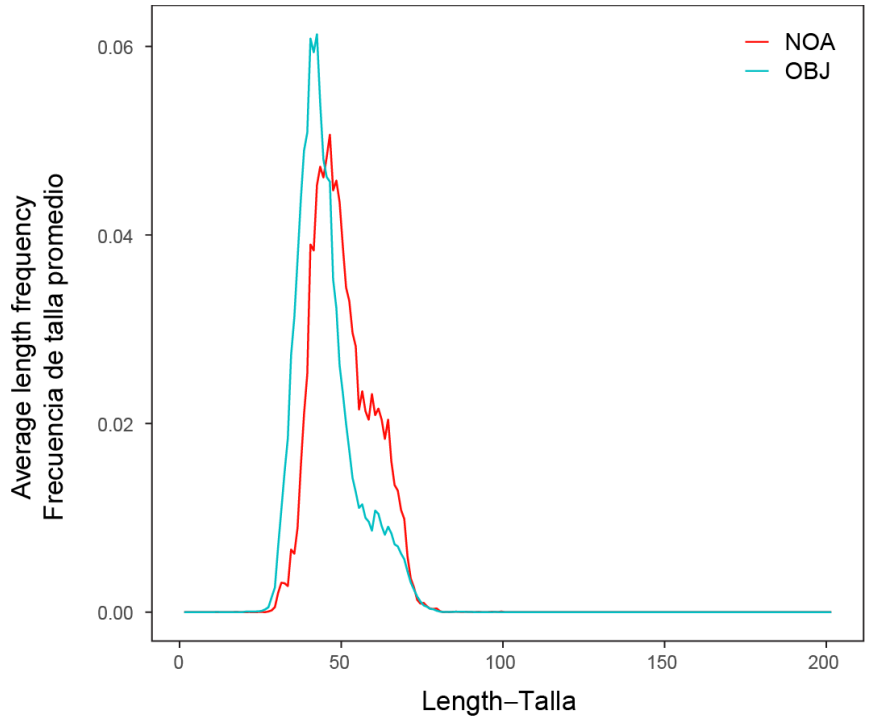

FIGURE 5. Average length frequency of SKJ caught by the OBJ and NOA sets in the EPO between 2000-2021.

FIGURA 5. Frecuencia de talla promedio de SKJ capturado en lances OBJ y NOA en el OPO durante 2000-2021.

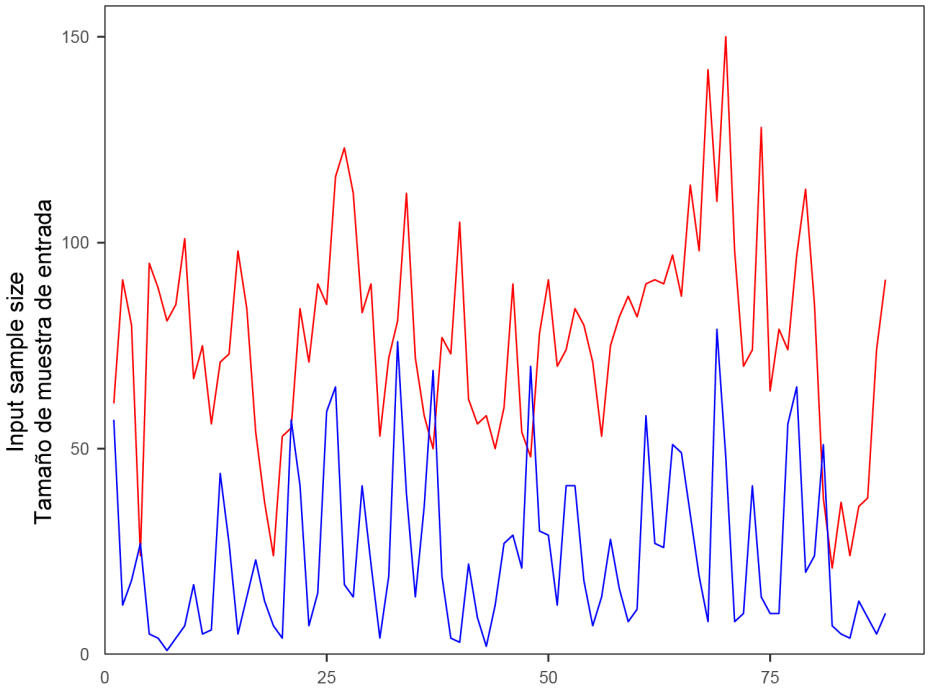

FIGURE 6. The input sample size of OBJ (red) and NOA (blue) length compositions for SKJ in the EPO.

FIGURA 6. Tamaño de muestra de entrada de las composiciones por talla OBJ (rojo) y NOA (azul) para el SKJ en el OPO.

TABLE 1. Standardized OBJ and NOA indices of abundance and the associated coefficients of variation (CV) for SKJ in the EPO.

TABLA 1. Índices de abundancia estandarizados OBJ y NOA y los coeficientes de variación (CV) asociados para el SKJ en el OPO.

Year	Quarter	Index (OBJ)	CV (OBJ)	NOA (OBJ)	CV (OBJ)
2000	1	2.053	0.077	1.504	0.140
2000	2	1.596	0.099	1.493	0.184
2000	3	0.873	0.104	0.769	0.199
2000	4	1.661	0.130	1.396	0.163
2001	1	1.412	0.076	0.232	0.236
2001	2	0.891	0.093	0.816	0.194
2001	3	0.851	0.089	0.328	0.256
2001	4	0.799	0.082	0.782	0.298
2002	1	0.994	0.082	0.471	0.252
2002	2	0.883	0.071	0.645	0.184
2002	3	0.669	0.070	0.517	0.210
2002	4	0.825	0.091	0.336	0.242
2003	1	1.129	0.067	0.748	0.182
2003	2	1.538	0.077	0.651	0.166
2003	3	1.628	0.076	0.478	0.209
2003	4	1.253	0.065	0.821	0.126
2004	1	1.216	0.063	0.728	0.161
2004	2	0.782	0.081	0.588	0.173
2004	3	0.569	0.077	0.680	0.192
2004	4	1.184	0.080	0.657	0.146
2005	1	1.536	0.064	0.931	0.149
2005	2	1.019	0.076	1.200	0.124
2005	3	1.108	0.076	0.738	0.230
2005	4	0.979	0.054	0.446	0.147
2006	1	1.182	0.058	0.676	0.127
2006	2	1.203	0.056	0.864	0.143
2006	3	1.293	0.053	0.956	0.177
2006	4	1.161	0.061	1.089	0.144
2007	1	1.036	0.059	0.941	0.143
2007	2	0.861	0.056	0.780	0.156
2007	3	0.692	0.065	0.683	0.217
2007	4	0.637	0.075	0.820	0.163
2008	1	1.221	0.061	1.299	0.119
2008	2	1.007	0.050	1.296	0.129
2008	3	0.811	0.056	1.185	0.178
2008	4	0.908	0.069	1.372	0.148
2009	1	0.898	0.060	1.158	0.124
2009	2	0.793	0.050	0.698	0.180
2009	3	0.742	0.055	0.740	0.205
2009	4	1.109	0.062	0.626	0.221
2010	1	1.208	0.054	0.780	0.167
2010	2	0.703	0.048	0.583	0.204

2010	3	0.704	0.058	0.526	0.224
2010	4	1.247	0.064	1.020	0.189
2011	1	1.448	0.067	0.988	0.167
2011	2	1.010	0.044	0.849	0.114
2011	3	0.782	0.051	1.622	0.168
2011	4	0.858	0.075	1.235	0.168
2012	1	0.856	0.076	0.965	0.135
2012	2	0.997	0.048	0.951	0.108
2012	3	0.989	0.055	1.022	0.195
2012	4	1.015	0.064	0.936	0.196
2013	1	1.155	0.056	1.262	0.139
2013	2	0.862	0.043	1.034	0.118
2013	3	0.670	0.055	0.919	0.188
2013	4	0.782	0.070	1.021	0.190
2014	1	0.815	0.057	1.042	0.126
2014	2	0.691	0.047	1.264	0.159
2014	3	0.851	0.056	1.199	0.171
2014	4	1.055	0.061	1.645	0.146
2015	1	0.969	0.051	1.221	0.129
2015	2	0.704	0.045	1.271	0.137
2015	3	0.945	0.057	0.590	0.219
2015	4	1.065	0.071	1.271	0.146
2016	1	0.843	0.055	0.678	0.173
2016	2	0.866	0.042	0.947	0.158
2016	3	0.991	0.051	0.945	0.202
2016	4	1.398	0.064	1.169	0.215
2017	1	1.103	0.046	1.216	0.150
2017	2	0.869	0.039	1.041	0.143
2017	3	0.626	0.048	0.814	0.196
2017	4	0.781	0.057	0.486	0.225
2018	1	0.802	0.047	0.968	0.132
2018	2	0.764	0.038	1.214	0.111
2018	3	0.667	0.049	1.100	0.180
2018	4	0.760	0.056	1.268	0.168
2019	1	0.772	0.046	1.241	0.137
2019	2	0.967	0.043	1.697	0.124
2019	3	0.990	0.058	1.548	0.154
2019	4	1.221	0.058	2.209	0.140
2020	1	1.319	0.042	1.568	0.116
2020	2	0.975	0.044	2.133	0.127
2020	3	0.818	0.051	1.053	0.182
2020	4	1.040	0.069	1.208	0.156
2021	1	1.080	0.049	1.247	0.120
2021	2	0.937	0.046	1.346	0.124
2021	3	0.793	0.046	0.987	0.167
2021	4	1.237	0.053	1.568	0.148